CTOBER 1, 1974, Volume 121, No. 1

NUIMA 121 (1) 1–203 (1974)

NUCLEAR INSTRUMENTS & METHODS

A JOURNAL ON ACCELERATORS, INSTRUMENTATION AND TECHNIQUES IN NUCLEAR PHYSICS

EDITOR: K. SIEGBAHN - UPPSALA

NORTH-HOLLAND PUBLISHING COMPANY — AMSTERDAM

NUCLEAR INSTRUMENTS AND METHODS 121 (1974) 491–498; © NORTH-HOLLAND PUBLISHING CO.

PORTABLE RADIOACTIVITY MONITOR FOR LIQUID EFFLUENTS, SURFACE CONTAMINATIONS, AND BULK SOLID WASTES*

C. J. UMBARGER and L. R. COWDER

Nuclear Analysis Research Group, University of California, Los Alamos Scientific Laboratory, Los Alamos, New Mexico 87544, U.S.A.

Received 30 July 1974

A versatile monitoring system is described which allows the nondestructive analysis of batch liquid samples, surface contaminations, and bulk waste packages for radioactive materials. The system uses the simplicity and extremely high sensitivity of NaI-based gamma-ray spectroscopy. As an example of the instrument's versatility, the simultaneous measurement of ^{235}U, ^{238}U, and thorium in liquids at sub-MPC (maximum permissible concentration) levels is described in detail. As a further demonstration of the system's capabilities, the assay of solid transuranic wastes at 10 nCi/g levels is discussed.

1. Introduction

With the increased awareness for environmental protection from human-produced radioactive contaminants, a need has arisen for appropriate monitoring devices that (1) are specific to the contaminants of interest, (2) have detectability limits below the desired monitoring level, (3) are simple to operate, and (4) have low acquisition cost. The instrument described fulfills all of these requirements for many radioactive materials (e.g., ^{241}Am, plutonium, uranium, ^{137}Cs, etc.) found in liquid effluents, surface contaminations ("spills"), and solid wastes. The instrument is portable and fieldable (can be battery-operated) and is sufficiently versatile to be capable of monitoring both batch liquid samples as well as bulk packages (e.g., $\approx$ 60 l boxes of transuranic wastes) with a single instrument. As a demonstration of the high sensitivity and specificity of the system, the simultaneous measurement of the two major isotopes of uranium (^{235}U and ^{238}U) and elemental thorium in liquid samples is described herein. As a further example of its usefulness, the analysis of solid waste materials containing plutonium and americium is also discussed.

2. Description of mechanical design

2.1. Liquid effluent monitor

The liquid assay system is designed to analyze batch liquid effluent samples contained in 250 ml plastic flasks[1]). The flasks are placed in the counting chamber shown in figs. 1 and 2. Once in the chamber the flask is pressed flush against a 127 mm diam. Na(I) detector (with a 0.25 mm Be entrance window) by steel springs. For best signal-to-background ratios, the detector thickness is chosen for the specific isotopes to be monitored. However, for general monitoring purposes, a 20 mm thick NaI is a good compromise between high detection efficiency and low backgrounds. (This particular size NaI is optimum for uranium and thorium analysis in liquids and will be discussed in detail below.) The thin Be window allows detection of low-

Fig. 1. Portable radioactivity monitor set-up in batch liquid monitoring mode. Samples in 250 ml plastic flasks are shown.

* Work performed under the auspices of the U.S. Atomic Energy Commission.

energy X-rays (≈ 16 keV) from plutonium and other heavy elements.

The detector shield is made of 22 mm thick lead contained by inner and outer brass tubes of 3.2 mm wall thickness (i.e., a "graded shield"). The back of the detector shield is made of two brass cones or cylinders with a 12.7 mm lead cone in between. Although the cone design adds to the fabrication costs, it considerably reduces the total mass of the instrument while maintaining adequate rear shielding for the detector. An additional polyethylene cone and ring (see fig. 2) provides insulation against mechanical and thermal shock for the detector during transportation. The face of the detector is covered by a 0.08 mm plastic sheet held to the detector assembly by the Plexiglas ring shown at the extreme left of fig. 2. This sheet assures easy cleaning of the detector face after assaying sample flasks with outer surface contaminations.

The cart and shield mounting box are made of welded aluminium, with the cart designed to disassemble into two pieces for ease of storage and transportation. The mounting box provides additional carrying space for four standard 102 by 51 by 203 mm lead bricks beneath the detector shield, providing an extra 51 mm of lead shielding between the detector and the floor. The shield face consists of an outer brass plate, 6.3 mm thick; a 25.4 mm thick lead plate; and an inner 3.2 mm copper plate. The instrument has a mass of approximately 68 kg and is surprisingly easy to maneuver. As shown in fig. 2, the entire shield housing disassembles easily into its many components and subassemblies for ease of shipment.

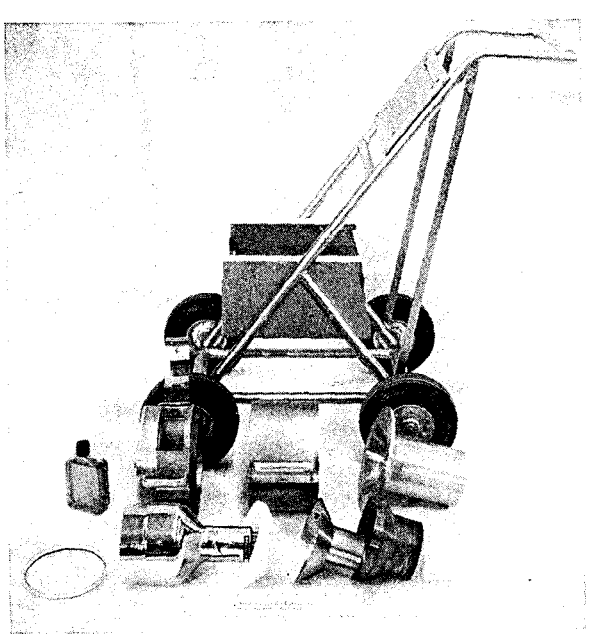

Fig. 2. Portable radioactivity monitor – exploded view.

2.2. Surface contamination and bulk solid waste monitor

For expanded versatility, the front counting chamber subassembly can be removed and the detector moved forward in a wide-angle viewing, or "snooper scope", configuration as shown in fig. 3. The monitoring of surface contaminations, large bulk packages, etc. can now be facilitated with no further modifications of the existing system. For horizontal surface monitoring, such as floor spills, the detector shield assembly must be mounted on gimbals to the cart.

3. Assay principle

The analysis for radioactive materials is carried out by measuring the intensity of gamma rays emitted from the sample and known to be specific to a particular radioactive species. After correcting for matrix absorption, branching ratios, specific activity of the isotope, and detection efficiency, the amount of radioactive material in the sample can be determined. A sometimes easier approach, and one that we have adopted, is the use of standards that closely resemble the unknown sample in matrix and radioactive material content. As a demonstration of the general assay principle and the possible uses and detectabilities that this system can achieve, we describe in detail below the analyses of liquid effluents for uranium and thorium content. In addition, we will also discuss the monitoring of low-density solid wastes (paper, cloth, plastic, incin-

Fig. 3. Portable radioactivity monitor set-up in surface contamination and solid waste assay mode.

erator ash, etc.) for americium and plutonium at 10 nCi/g levels.

3.1. Analysis for uranium and thorium in liquid effluents

The liquid samples are contained in the 250 ml plastic flasks discussed previously and placed in the liquid sample counting chamber. The analysis for ^{235}U is accomplished by measuring the intensity of the 185.7 keV gamma ray[2]) emitted immediately following ^{235}U alpha decay to ^{231}Th. This gamma ray is very prolific, its emission rate[3]) being $\approx 4.3 \times 10^4$/g s and is independent of the time since the uranium was chemically purified. A typical gamma-ray spectrum is shown in fig. 4. The sample contained 0.25 g uranium of 2% enrichment. The various gamma-ray regions are labeled.

Quantitative measurement for ^{238}U is performed by monitoring the intensity of the ≈ 63 keV gamma-ray doublet[3]) found in the nucleus ^{234}Pa, a granddaughter of ^{238}U. After uranium chemical separation, this doublet exhibits a 24.1 d half-life for activity grow-in since they follow the beta decay of ^{234}Th, the daughter of ^{238}U. As shown in fig. 4, this photon energy region is relatively clean and well resolved from the L and K X-ray regions of the uranium daughters. The intensities of the X-ray regions (≈ 16 keV and ≈ 95 keV, respectively) not only exhibit time depen-

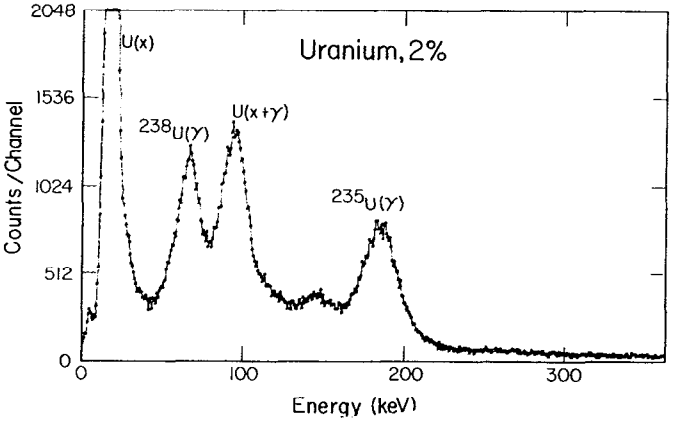

Fig. 4. Typical uranium spectrum measured with portable radioactivity monitor and a multichannel analyzer. The major peaks of interest are identified as to daughter X-ray or γ-ray origin in a uranium isotope or element (if due to more than a single isotope). The sample contained 250 mg uranium (2% enrichment) in 250 ml of water.

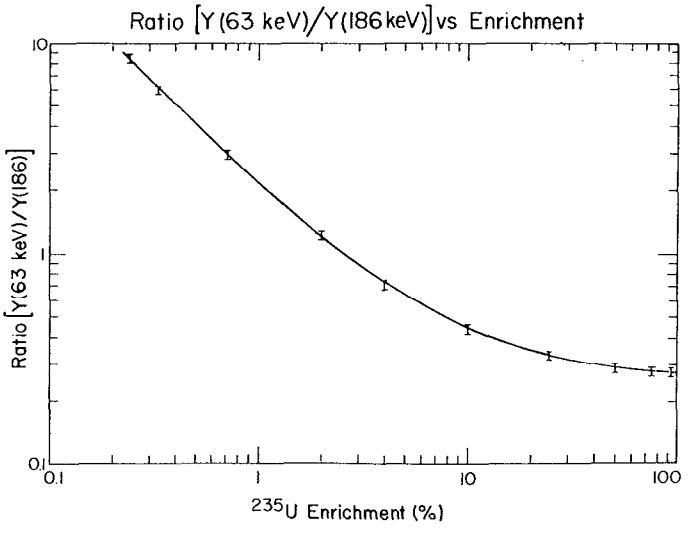

Fig. 5. Ratio of signals in 63 keV region to that in the 186 keV region vs uranium enrichment. The indicated error bars are $\pm 5\%$ and are for reference only. The solid line is the result of a computer least-squares fit.

dence as daughters grow in, but are also composites of ^{235}U and ^{234}U activities (gamma and X-rays), besides ^{238}U, hence complicating enormously the data analysis. This is magnified by the general lack of knowledge of the $^{235}U/^{234}U$ ratio, which varies between 100 and 200. For these reasons, the 63 keV region is chosen for ^{238}U analysis. It is essentially a clean ^{238}U signature, albeit time-dependent.

By measuring the ratio of the intensity of the signal in the 63 keV region to that in the 186 keV region, a signature of the uranium enrichment $[^{235}U/(^{235}U+^{238}U)]$ results. [Because of the very low uranium concentrations in the sample, the usual "enrichment meter" principle[4]) of monitoring only the 186 keV gamma ray cannot be applied.] An enrichment calibration curve was obtained by using standard solutions of various enrichments spanning the enrichment region of interest, as shown in fig. 5. Although this enrichment signature has the time dependence of the 63 keV gamma ray, this is not as deleterious as first appears. Fig. 6 shows this signature as a fuction of time, after chemical separation, relative to its equilibrium value. After a wait of only 41 d, the enrichment error is less than 30%. This error is a positive bias toward higher enrichments. In many instances the uranium solutions being analyzed may be known to have an age exceeding a given time period, hence allowing a maximum enrichment error to be assigned. In addition, a large enrichment error, e.g., $\pm 50\%$, is probably not unreasonable for low level, ~MPC, effluent streams.

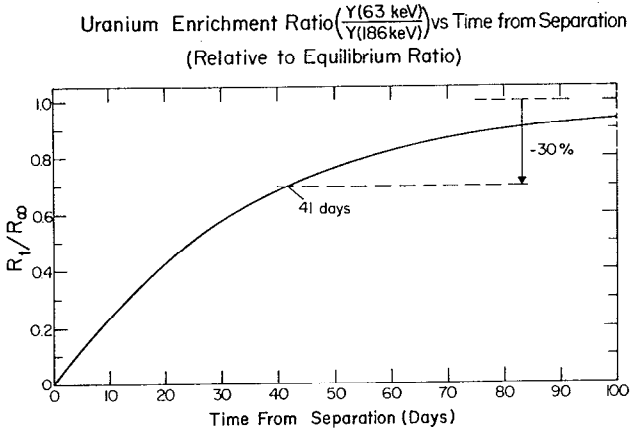

Fig. 6. Calculated uranium enrichment ratio as a function of time since uranium chemical purification. The time dependence is due to the 24.1 d half-life of ^{234}Th, which produces the 63 keV gamma ray used for ^{238}U analysis.

Analysis for thorium is accomplished by monitoring the intensity of the 238 keV gamma ray found deep in the decay chain of ^{232}Th (see fig. 7 for a typical thorium spectrum). This gamma ray is actually found in the nucleus ^{212}Bi, which is a direct daughter of ^{212}Pb [2]). Although the intensity of this gamma ray is dependent on the time since thorium chemical separation, one is still able to obtain a reasonable estimate of the thorium content regardless of age, if a 43% error is acceptable. Figs. 8 and 9 show the intensity of this gamma ray as a function of time since thorium separation relative to its equilibrium intensity. The calculations[5]) assume only a chemical separation of thorium, not isotopic; i.e., at $t=0$ both ^{232}Th and ^{228}Th are present. If the thorium calibration curve is based on 70% of the equilibrium activity of the 238 keV gamma ray, then the maximum assay error is $\pm 43\%$ after a 3 d wait since separation (see figs. 8 and

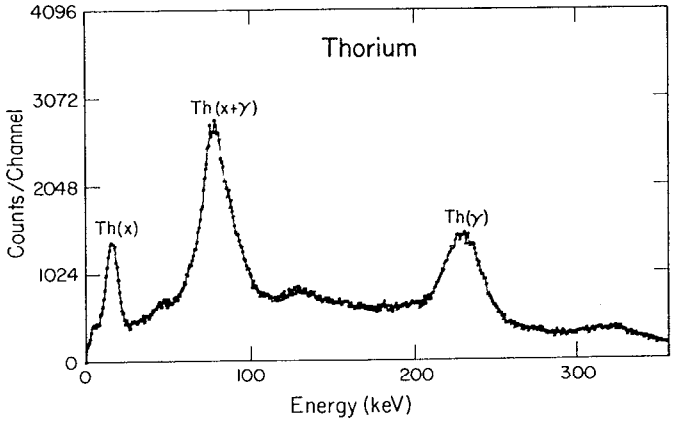

Fig. 7. Typical thorium spectrum measured with portable radioactivity monitor and a multichannel analyzer. The major daughter peaks of interest are identified. The sample contained 250 mg thorium in 250 ml of water. The thorium was in equilibrium with its daughters.

Fig. 8. Calculat

9). Of course
more accurat
As shown
bration curv
of ≈ 0.27 at h
This is cause
ray[3]) from
Due to the in
certain fracti
counted in
detector wou
complexity a
quickly this
at high enric

Thorium (

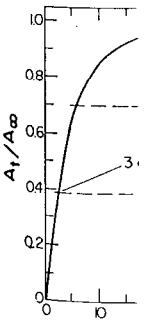

Fig. 9. Calculat
librium activity
chemical, but n
are

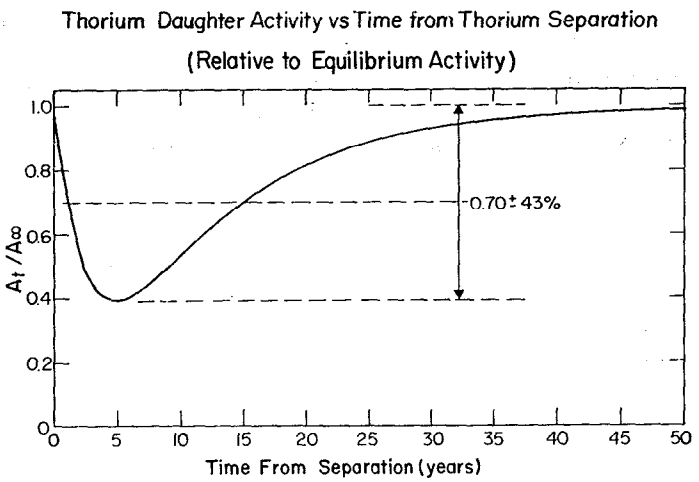

Fig. 8. Calculated thorium daughter activity, relative to its equilibrium activity, as a function of time (years) since thorium chemical, but not isotopic, separation. The extremes of the curve are ±43% of 70% of the maximum value.

9). Of course, if the age of the solution is known, a more accurate assay is possible.

As shown in fig. 5, the uranium enrichment calibration curve levels off to a constant intensity ratio of ≈ 0.27 at high uranium enrichment values ($E \gtrsim 75\%$). This is caused by interference from a 53 keV gamma ray[3]) from ^{234}U (which tracks the ^{235}U content). Due to the imperfect resolution of the NaI detector a certain fraction of the 53 keV gamma ray yield is counted in the 63 keV ^{238}U window. [A Ge(Li) detector would eliminate this interference but add complexity and cost to the overall system.] How quickly this enrichment calibration curve levels off at high enrichments depends on the energy resolution of the particular NaI detector used and the width of the integration window selected for the 63 keV region (this assumes that gamma-ray spectrum peak stripping capability is not available). The decision on window width for the 63 keV region is based on the maximum enrichment one needs to measure and the counting times available for adequate statistics. The window widths chosen for the present data are 47–77 keV, 163–208 keV, and 219–258 keV for the 63 keV, 186 keV, and 238 keV regions, respectively. Due to the uncertainty in the $^{234}U/^{235}U$ ratio, the interference of the 53 keV gamma ray with the 63 keV integration region introduces a ≈ ±3% error in the enrichment measurement.

In a typical assay signal backgrounds are subtracted in two steps. First a clean water sample is assayed to obtain general room backgrounds in the three regions of interest, as well as a fourth region used for "real-time" background analysis. This last region, which lies above the 238 keV area and stretches from 264 to 312 keV, is used to correct for backgrounds in the 186 and 238 keV regions due to Th and U contributions, respectively. The correction factor for this real-time background subtraction was obtained by measuring pure uranium and thorium solutions. Accordingly, the appropriate backgrounds for the 186 and 238 keV regions were determined to be 1.87 and 1.21 times the signal (room background subtracted) in the fourth integrated region (264–312 keV), respectively. Such a prescription for background subtraction was found necessary to produce linear ^{235}U and thorium responses over a wide range of uranium enrichment and uranium/thorium values.

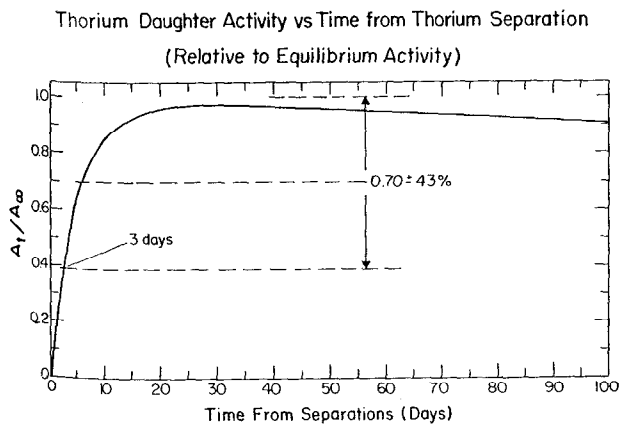

Fig. 9. Calculated thorium daughter activity, relative to its equilibrium activity, as a function of time (days) since thorium chemical, but not isotopic, separation. The extremes of the curve are ±43% of 70% of the maximum value.

In order to assay for uranium enrichment when thorium is present, a final correction is necessary for the background from thorium in the 50–100 keV region, as shown in fig. 7. The thorium signal in this region is essentially due to K X-rays and gamma rays from daughter products of thorium. One first assays for thorium in the sample and then removes the appropriate background in the 63 keV ^{238}U region. For the samples assayed here, it was found necessary to remove 1.15 times the signal in the 238 keV region from the 63 keV region. The yield remaining is essentially a pure ^{238}U signal. Because of the thorium interference with the ^{238}U signal, a thorium/uranium ratio of $\leq 4/1$ is necessary for accurate enrichment measurements. Where the uranium enrichment is known, this ratio can probably go as high as 10/1 with good assay results for ^{235}U alone and thorium.

Typical electronics needed for data acquisition consists of a high voltage power supply (1 kV) and a multichannel analyzer (MCA) with built-in amplifier. An MCA with "intensified region" capability and a region integration feature is ideal. The four regions of interest discussed above can be programmed into the MCA with the aid of three standard calibration samples; one uranium of known enrichment and content, one thorium, and one pure water for room background subtraction purposes. Portable battery-powered instrumentation (see fig. 1) can also be used, but with concomitant loss in electronic stability, flexibility, and ease of calibration and operation.

The counting efficiency for 63, 186, and 238 keV gamma rays emitted from the sample flask is constant at $\approx 26\%$ over the concentration range of 0–1 g uranium (or thorium) per liter. Above 1 g/l this efficiency begins to drop off due to self-absorption in the sample, as verified both by experiment and calculation[6]). (The upper concentration range can be extended by changing to thinner sample flasks.) Approximate signal counting rates for ^{235}U (186 keV), ^{238}U (63 keV, at equilibrium), and thorium (238 keV, at equilibrium) are $\approx 1.1 \times 10^4$/s g, $\approx 2.1 \times 10^2$/s g, and $\approx 2.5 \times 10^2$/s g, respectively.

Detectability limits for uranium and thorium are shown in table 1. This limit is based on a signal equal to three standard deviations (3σ) of the room background for a 1000 s counting period. The system has demonstrated detectabilities far below MPC [7]) levels for ^{235}U and ^{238}U, and at the 0.1 MPC level for thorium. [At lower elevations than where these measurements were performed (2225 m), the detectabilities should improve considerably due to reduced cosmic ray backgrounds.] The detectability limit for thorium in terms of MPC units can vary because of uncertainties in the specific activity of natural thorium samples caused by possible escape of daughters from the material. This points up one area of concern for thorium assay with this system, since the thorium analysis is based on the measurement of a daughter activity with the assumption that no daughters have escaped (natural separation) after the original chemical (artificial) separation. If daughter escape occurs, the assay results will be lower than the actual thorium content.

TABLE 1
Detectability limits for uranium and thorium in water.

Isotope	MPC[a] (μCi/cm^3)	MPC[a] (μg/cm^3)	Detectability[b] (μg/cm^3)	Detectability[b] (MPC)
^{235}U	3×10^{-5}	14	0.08	0.006
^{238}U	4×10^{-5}	120	3.0	0.03
Th (Nat)	2×10^{-6}	18	3.0	0.17

[a] Public water systems, ref. 7.
[b] 1000 s count, 3σ level above background.

An additional concern with thorium assay is that the sample may contain recycled uranium fuel with significant amounts of ^{232}U. This isotope of uranium decays to ^{228}Th and, hence, enters the normal thorium decay chain. When ^{232}U is present, it will result in an erroneous thorium assay. If the recycled uranium contains ^{237}U, it too will have a deleterious effect on the uranium–thorium measurement due to interference from its 208 keV gamma ray. However, if the material can be stored for a month or more, this isotope may be reduced to an acceptable level because of its short 6.7 d half-life.

If other radioactive materials are present, such as fission products, etc., the detectability for uranium and thorium will be degraded due to increased backgrounds. If an MCA is used for data acquisition, any significant amount of such materials will be evident, with that particular sample being tagged for more extensive analysis.

The aforementioned concerns about interference from other radioactive materials points up the one major limitation of this assay system. As with any NaI based instrument, "black box" measurements can yield erroneous results. For such cases the use of a Ge(Li) detector may determine possible interferences. However, in the vast majority of assays performed in fuel process and fabrication facilities the samples are generally well characterized, with possible contaminants

TABLE 2

Typical assay results for mixed uranium–thorium solutions.

Sample	Thorium Mass (mg)	Thorium Assay (mg)	Thorium Δ (%)	Uranium-235 Mass (mg)	Uranium-235 Assay (mg)	Uranium-235 Δ (%)	Enrichment ^{235}U Real (%)	Enrichment ^{235}U Assay (%)	Enrichment ^{235}U Δ (%)	Th/U
1	51.7	53.5	3.5	2.0	2.05	2.4	4.0	4.05	1.2	1.03
2	206.7	208.6	0.9	2.0	2.00	0.0	4.0	3.65	8.7	4.13
3	206.7	206.1	0.3	14.0	14.02	0.1	50.0	36.5	27.0	7.38

known in advance from a working knowledge of the facility's feed and product materials.

Assay accuracy of $\pm 10\%$ is routinely possible for ^{235}U, ^{238}U (enrichment), and thorium content if daughter equilibrium can be assured for ^{238}U and thorium; otherwise the errors stated in the text are appropriate. This $\pm 10\%$ error applies to uranium enrichment of $\approx 10\%$ or less. Above $\approx 10\%$ enrichment, the leveling off of the calibration curve (see fig. 5) affects larger errors. As discussed earlier, a narrower integration window for the 63 keV gamma-ray region will increase the accuracy of the enrichment measurement above 10% enrichments, but at a sacrifice in counting times. Also, for accurate enrichment measurements, the thorium/uranium content should be ≤ 4 to reduce thorium-related backgrounds in the ^{238}U, 63 keV, assay region. This large thorium-related background produces large errors for enrichments, as shown in table 2 for typical assay results obtained from mixed uranium–thorium solutions. As also shown in table 2, good enrichment assay results are possible for thorium/uranium ratios of ≈ 4. For reasonable thorium/uranium ratios ($\leq 10/1$) the accuracy of the ^{235}U and thorium assays seems unaffected by the presence of each other and have errors of $\leq 10\%$.

3.2. Analysis for americium and plutonium at 10 nCi/g in solid wastes

According to the recently released AEC Manual Chapter 0511 (Radioactive Waste Management)[8]), transuranium-contaminated solid wastes are *those contaminated with certain alpha-emitting radionuclides of long half-life and high specific radiotoxicity to greater than 10 nCi/g....* The radionuclides included are plutonium, and transplutonium nuclides except ^{238}Pu, and ^{233}U and its daughter products. The 10 nCi/g level is a criterion for choosing different means of handling different activity levels of transuranium-contaminated solid wastes. Accordingly a monitoring scheme is needed for measurements at and below this activity level; but, due to the very low natural radiation yields (spontaneous fission neutrons and high energy gamma rays) at such activity levels, a different approach than the more conventional assay systems is needed[9]).

Because the L X-ray yields of the transuranic materials are the most prolific natural signature[9]) (except for weakly penetrating alpha particles), the assay principle that has been adopted is actually a hybrid[10]) of a high energy gamma-ray detection scheme coupled to one detecting X-rays. This multienergy gamma assay principle allows one to monitor the X-ray region for the sub-10 nCi/g wastes, subsequently crossing over to progressively higher energy gamma rays as the activity level increases. Such a hybrid system combines the high sensitivity (and relatively poor accuracy) of X-ray detection at the 10 nCi/g level with the lower sensitivity, but improved accuracy, of gamma-ray detection at higher activity levels. The errors referred to here are due to absorption by the matrix material and self-shielding by the transuranics themselves. The self-shielding effects are severe for all photon energies considered here, particularly for the low energy L X-rays[11]). Part of the self-shielding problem can be alleviated by using proper standards (e.g., dried liquid plutonium standards for assaying process line-generated wastes from ion-exchange columns). Also, for typical room-generated wastes which are reasonably free of contamination, essentially no self-absorption effects exist.

The detector and shield are the same as described earlier. The 0.25 mm Be entrance window is thin enough to allow X-ray transmission into the crystal, whereas the detector itself is thick enough to appreciably absorb high-energy gamma rays; e.g., 400 keV complex from ^{239}Pu [3]). For improved 400 keV gamma-ray detection efficiency a 50.8 mm thick NaI(Tl) detector can be utilized[10]). The geometrical configuration is similar to that shown in fig. 3, but with the large package being rotated and translated

vertically past the detector with a 25 mm × 100 mm iron collimator. The combination of rotation and collimation tends to smooth the response of the spacially distributed radioactive materials.

As reported previously[10–13]) the detectability of the system is less than 10 nCi/g for bulk packages (e.g., 60 l) of low density (combustibles, such as paper, cloth, plastic, etc.) wastes. For such packages, containing approximately 4 kg of wastes, detectability limits (3σ above background) of 0.04 nCi/g are possible in a 1000-s count monitoring the 16 keV L X-ray region[12]). This is equivalent to ≈ 2 μg Pu (6% ^{240}Pu) in 4 kg of waste. By monitoring the higher energy photon regions of plutonium (120 keV, 200 keV, and 400 keV), detectability limits of 3.4 nCi/g, 27 nCi/g, and 36 nCi/g are achieved in 1000 s, respectively[12]). The detectability limit for ^{241}Am (monitoring its 60 keV gamma ray) is approximately 15 times lower (better) than that of plutonium using the L X-ray region (16 keV). This is due to the higher photon yield per disintegration for ^{241}Am compared to ^{239}Pu and to the increased penetrability of the ^{241}Am 60 keV γ-ray compared to the 16 keV X-ray. Plutonium assay errors are typically ±50% using L X-rays, and ±30% for gamma-ray measurements. Smaller packages than the 60 l container would afford smaller errors. These errors statements assume that adequate reference standards can be prepared; otherwise the errors could be considerably larger.

The authors wish to thank Drs R. A. Forster and D. A. Close for performing the Monte Carlo calculations for the detection efficiency and the least-squares computer fit used in fig. 5.

References

1) No. 3024 Tissue Culture Flask, Falcon Plastics, 19[illegible] Williams Dr., Oxnard, CA 93030.
2) C. M. Lederer, J. M. Hollander and I. Perlman, *Table of isotopes* (6th ed.; J. Wiley, New York, 1967).
3) J. E. Cline, Idaho Nuclear Corp. report IN-1448 (1970).
4) T. D. Reilly, R. B. Walton and J. L. Parker, Los Alamos Scientific Laboratory report LA-4605-MS (1970).
5) See also L. V. East, Los Alamos Scientific Laboratory report LA-5291-PR (1973).
6) R. A. Forster and D. A. Close, private communication.
7) United States Code of Federal Regulations, Title 10 (Atomic Energy), Part 20 (Standards For Protection Against Radiation) (1968); and United States Atomic Energy Commission Manual Chapter 0524 (Standards For Radiation Protection) (1968).
8) United States Atomic Energy Commission Manual Chapter 0511 (Radioactive Waste Management) (1973).
9) C. J. Umbarger and R. A. Forster, Los Alamos Scientific Laboratory report LA-5291-PR (1973).
10) C. J. Umbarger and R. A. Forster, Los Alamos Scientific Laboratory report LA-5431-PR (1973).
11) R. A. Forster and C. J. Umbarger, Nucl. Instr. and Meth. **117** (1964) 597.
12) C. J. Umbarger, Los Alamos Scientific Laboratory report LA-5557-PR (1973).
13) C. J. Umbarger and R. A. Forster, Trans. Am. Nucl. Soc. **17** (1973) 332.